A New 2-D Inversion Scheme For Magnetotelluric Data Using A Modified RRI Method

Ki Ha Lee[1], Ganquan Xie[1], Kazunobu YAMANE[2] and Shinji TAKASUGI[2]

1 Lawrence Berkeley Laboratory, California, U.S.A

2 Geothermal Energy Research and Development Co.,LTD., Tokyo, Japan

key *words* : magnetotellurics, inversion, geothermal exploration

Abstract

A new two-dimensional (2D) magnetotelluric (MT) inversion scheme is proposed in this paper. This scheme is based on a locally two-dimensional analysis in order to minimize computational time and computer memory.

The MT governing equation is linearized in terms of the magnetic field and electrical conductivity for the perturbation analysis. The perturbed equation is then multiplied by a test function and integrated over the cross section. Integrating by parts and then substituting this test function with local magnetic fields, a new equation is obtained that is a 2-D variational integral for the electrical conductivity. The new equation is general in the sense that it can explicitly include the horizontal derivative of the magnetic field. If the horizontal derivative term is eliminated, the new equation becomes identical to the Rapid Relaxation Inversion (RRI) scheme proposed by Smith and Booker(1991).

Introduction

The magnetotelluric (MT) method has been successfully applied to geothermal exploration for many years. Recently, many useful 2-D MT inversion schemes have been developed. Among the many studies reported, the Occam inversion, presented by deGroot-Hedlin and Constable (1990). may be one of the most rigorous non-linear approaches which calculates the 2-D Frechet derivative, and the Rapid Relaxation Inversion scheme (RRI), by Smith and Booker (1991). is one of the best approximate methods. While the Occam's inversion scheme may produce reliable inverse solutions, it takes enormous computational time and computer-memyry. This immense computing resource may be an too large obstacle to overcome for many people. The RRI method provides reasonable solutions, with less computing resources, because partial derivatives are obtained from a perturbation analysis which uses only the cross terms of the horizontal gradient. Careful attention must be paid in handling MT data, especially the TM-mode, which is liable *to* static effects. The inversion scheme presented here is quite new as it falls between the extremes represented by the Occam and RRI methods.

While this new inversion scheme does not require additional computation time when compared with the original RRI scheme, it nevertheless provides a higher resolution MT profile without a great deal more of user involvement in adjusting the model dependent parameters in the code and input data. This method involves a locally 2-D analysis (the inversion part of the original RRI method is strictly one-dimensional) and is somewhat similar to the block-like Gauss-Scidel relaxation method. Except for electric and cultural noise it does not require topographic and static effect corrections on the data and should be able to operate directly on the field data. This particular ability is useful in comparison with the original RRI method since it minimizes efforts involved in preconditioning the data which usually requires a great deal of careful data handling processes. The algorithm for this new inversion scheme, named GRRI (Generalized Rapid Relaxation Inversion), is now prcscnted.

Theoretical description

For comparison we first review the original RRI algorithm. Maxwell's equation used in the RRI inversion algorithm for the TM-modc MT field (Smith et. al., 1990) is

$$\frac{\partial}{\partial x}\left(\frac{1}{\sigma}\frac{\partial H_y}{\partial x}\right)+\frac{\partial}{\partial z}\left(\frac{1}{\sigma}\frac{\partial H_y}{\partial z}\right)-i\omega\mu H_y=0$$

First, introducing the variable U (with the subscript 'y' dropped from the magnetic field)

$$U=\frac{1}{\sigma H}\frac{\partial H}{\partial z} \qquad (2)$$

equation(1) is modified to

$$\frac{\partial U}{\partial z} + \sigma U^2 + \frac{1}{H}\frac{\partial}{\partial x}\left\{\frac{1}{\sigma}\frac{\partial H}{\partial x}\right\} - i\omega\mu = 0 \qquad (3)$$

Then, following a perturbation analysis, this non-linear equation is approximately linearized as

$$\frac{a}{az}\delta U + 2\sigma_0 U_0 \delta U + U_0^2 \delta\sigma = 0 \qquad (4)$$

for which the solution for the conductivity variation is obtaincd by solving the integral

$$\delta U(x_i, 0) = \int \left[\frac{1}{\sigma_0(x_i, z)\, H_0(x_i, 0)}\frac{\partial H_0(x_i, z)}{\partial z}\right]^2 \delta\sigma(x_i, z)\, dz \qquad (5)$$

Thc approximation resulting from the elimination of the lateral term in equation (2) leads to a one-dimensional solution. This approximation may be acceptable in cases of TE-mode inversion (for the TE-mode formula see Smith and Booker,1991) because there arc no surface charges and therefore no channeling. But it could result in serious distortions lor cases of TM-mode inversion. To include current channeling across inhomogeneous boundaries, in order to handle static effects directly, the following generalized algorithm has bccn implemented.

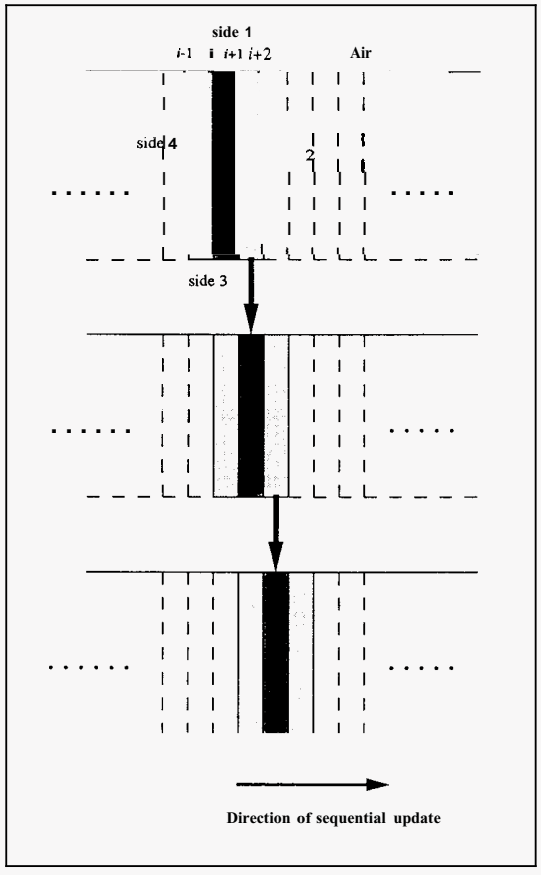

Figuer 1 Schematic diagram of GRRI's sequential conductivity update

To generate Frechet derivatives (somctimcs called the "Sensitivity Function") a perturbation (6) is introduced to equation (1).

$$\frac{\partial}{\partial x}\left[\delta\left(\frac{1}{\sigma}\frac{\partial H}{\partial x}\right)\right] + \frac{\partial}{\partial z}\left[\delta\left(\frac{1}{\sigma}\frac{\partial H}{\partial z}\right)\right] - i\omega\mu\delta H = 0 \qquad (6)$$

Next, we multiply this equation by a test function H* and integrate over a domain consisting of three vertical columns of the mesh uscd for the inversion (see Figure 1).

$$\int_\Omega \left\{\frac{\partial}{\partial x}\left[\delta\left(\frac{1}{\sigma}\frac{\partial H}{\partial x}\right)\right]H^* + \frac{\partial}{\partial z}\left[\delta\left(\frac{1}{\sigma}\frac{\partial H}{\partial z}\right)\right]H^* - i\omega\mu\delta H H^*\right\} d\Omega = 0 \qquad (7)$$

Integrating by parts, the equation is reduced to

$$\int_{\partial\Omega} \delta\left(\frac{1}{\sigma}\frac{\partial H}{\partial n}\right)H^* dl - \int_\Omega \left\{\frac{1}{\sigma}\left[\frac{\partial\delta H}{\partial x}\frac{\partial H^*}{\partial x} + \frac{\partial\delta H}{\partial z}\frac{\partial H^*}{\partial z}\right] + i\omega\mu\delta H H^*\right\} d\Omega$$

$$= -\int_\Omega \frac{\delta\sigma}{\sigma^2}\left[\frac{\partial H}{\partial x}\frac{\partial H^*}{\partial x} + \frac{\partial H}{\partial z}\frac{\partial H^*}{\partial z}\right] d\Omega \qquad (8)$$

where the normal derivative $\partial/\partial n$ in the first integral is equivalent to $-\partial/\partial z$, $\partial/\partial x$, $\partial/\partial z$ and $-\partial/\partial x$ for sides 1, **2**, **3** and **4**, respectively (Figure 1).

At this point we choose the test function H^* to bc zero cverywhcrc except for the area covered by the chosen domain in which

$$H^*(x_{i-1}, z_j) = H^*(x_{i+2}, z_j) = 0.0$$
$$H^*(x_i, z_j) = H(x_i, z_j),\quad H^*(x_{i+1}, z_j) = H(x_{i+1}, z_j)$$

Substituting this test function and the appropriate normal derivatives into equation (8) results in

$$\int_{x_{i-1}}^{x_{i+2}} \left[\delta\left(\frac{1}{\sigma}\frac{\partial H}{\partial z}\right)H^*\right]_{z=0} dx + \int_\Omega \left\{\frac{1}{\sigma}\left[\frac{\partial\delta H}{\partial x}\frac{\partial H^*}{\partial x} + \frac{\partial\delta H}{\partial z}\frac{\partial H^*}{\partial z}\right] + i\omega\mu\delta H H^*\right\} d\Omega$$

$$= \int_{\Omega} \frac{\delta\sigma}{\sigma^2}\left[\frac{\partial H}{\partial x}\frac{\partial H^*}{\partial x} + \frac{\partial H}{\partial z}\frac{\partial H^*}{\partial z}\right] d\Omega \qquad (10)$$

In ordcr to implement this Last equation to find $\delta\sigma_k$(k indicates the k-th iteration), only two initial inversion iteration solutions for **k = 1** and 2 are necessary using the RRI mcthod. Then the left hand side of the equation can be estimated iteratively using these two initial solutions. The right hand side of the equation can be divided into three sections:

$$\int_{\Omega_1} \frac{\delta\sigma}{\sigma^2}\left[\frac{\partial H}{\partial x}\frac{\partial H^*}{\partial x} + \frac{\partial H}{\partial z}\frac{\partial H^*}{\partial z}\right] d\Omega, \quad \text{for} \quad x_{i-1} < x < x_i \qquad (10\text{-}1)$$

$$\int_{\Omega_2} \frac{\delta\sigma}{\sigma^2}\left[\frac{\partial H}{\partial x}\frac{\partial H^*}{\partial x} + \frac{\partial H}{\partial z}\frac{\partial H^*}{\partial z}\right] d\Omega, \quad \text{for} \quad x_i < x < x_{i+1} \qquad (10\text{-}2)$$

$$\int_{\Omega_3} \frac{\delta\sigma}{\sigma^2}\left[\frac{\partial H}{\partial x}\frac{\partial H^*}{\partial x} + \frac{\partial H}{\partial z}\frac{\partial H^*}{\partial z}\right] d\Omega, \quad \text{for} \quad x_{i+1} < x < x_{i+2} \qquad (10\text{-}3)$$

The integral in domain R_1 can be evaluated since the conductivity variation in that domain has just been calculated through the identical process that started from the left-most column and continues in the positive x-direction For the evaluation of the integral in domain R3 we can use the conductivity variation obtained and used in the last iteration $\delta\sigma_{k-1}$. The only unknown is then the variation $\delta\sigma_k$ in domain Ω_2. Following these steps, we may finally simplify equation (10) to

$$\int_{\Omega_2} \frac{\delta\sigma}{\sigma^2}\left[\frac{\partial H}{\partial x}\frac{\partial H}{\partial x} + \frac{\partial H}{\partial z}\frac{\partial H}{\partial z}\right] d\Omega = S(\sigma, H, \frac{\partial H}{\partial x}, \frac{\partial H}{\partial z}); \quad \text{with} \quad x_i < x < x_{i+1} \qquad (11)$$

where the right hand side is the source function consisting of all the integrals mentioned above.

The new equation (11) is general in the sense that it can explicitly include the horizontal derivative of the magnetic field within the model. If the horizontal derivative term is eliminated and both sides are divided by the **square** of the surfacc magnetic field (H^2_0constant), the new equation becomes identical to the old one (equation (5)).From this simple analysis it can be said that the old RRI algorithm is a special case of the more general new formula for GRRI.

Inversion with Topography

It can be shown that the GRRI scheme is also well suited for inverting data with topography, particularly for the TM-mode, since the core of the algorithm is 2-D (i.e. the horizontal derivative of the magnetic field is uscd **as** a part of the functional to be minimized). In the new scheine data are incorporated in the first term of equation (8), and in the presence of topography the term will be modified to (Figure 2)

$$-\int_{\xi_{i-1}}^{\xi_{i+2}} \left[\delta\left(\frac{1}{\sigma}\frac{\partial H}{\partial \eta}\right) H\right]_{\text{surface}} d\xi \qquad (12)$$

Herc the normal derivative $\partial/\partial n$ in the first integral is equivalent to $-\partial/\partial\eta$ on the inclined surface (side 1). It is assumed that the same convention for the test function applies to this equation. As can be seen from Figure 2 the surface can be of any topography. The electric fields used are tangential (in the ξ-direction) to the surfacc. It is consistent with the way the electric field is measured using an electric dipole.

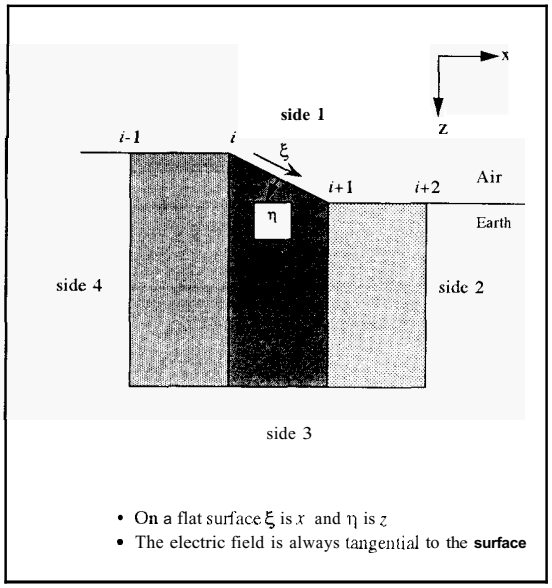

Figure 2. Model with topography

Examples

Synthetic Data

The algorithm was tested using a model with topography, and with imhomogeneities at depth as well as on the surface (Figure **3)** The electric dipoles of this model are continuous The results (Figure **4)** show that there is a little noise below the hill and valley and the image of the buried conductor below the hill is pulled up a little and the resistive body under valley pulled down.

However, the inversion results are good considering that there is topography on the surface and the bottom half space is conductive. Next, in spite of the fact that the size of surface conductor is relatively large, the inversion very nearly recovers the exact surface conductor as used in the input model. The inversion does not need static correction and, therefore, it should be suitable for directly interpreting field data as a routine process.

Field data

This new method was applied to two CSMT/MT survey lines lying within the Sumikawa area in the Akita Prefecture in Japan (Figure **5).** Beneath the Quaternary andesite lava which covers this area are pyroclastic rocks and shale. Underlying this sequence is pre-Tertiary granodiorite. **The** clcctric dipoles of the CSMT survey are continuous along the

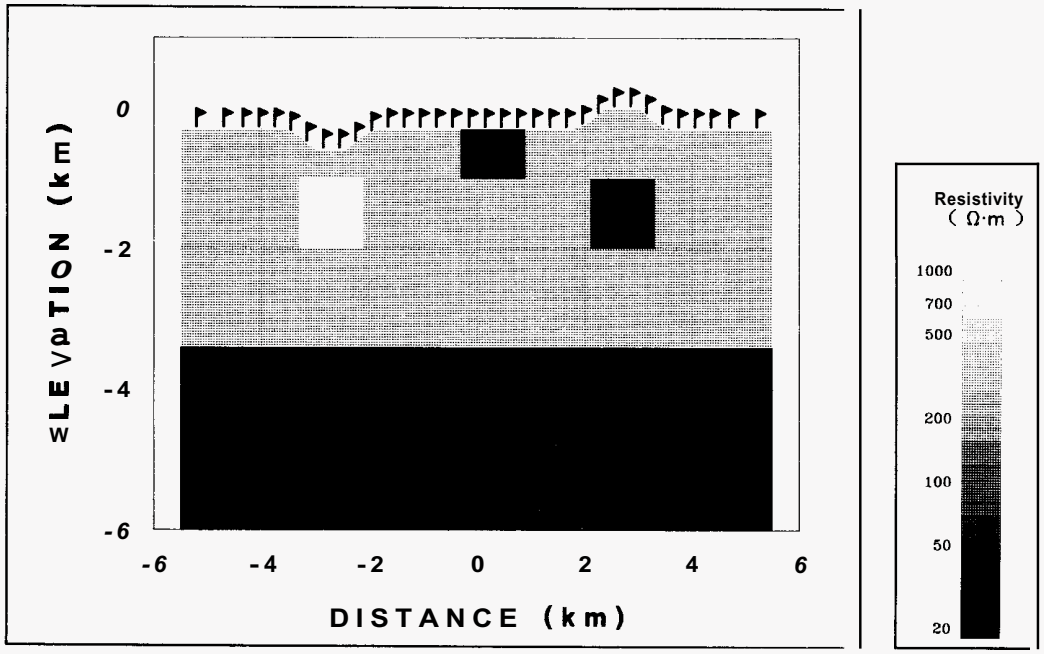

Figure **3.** Model for testing

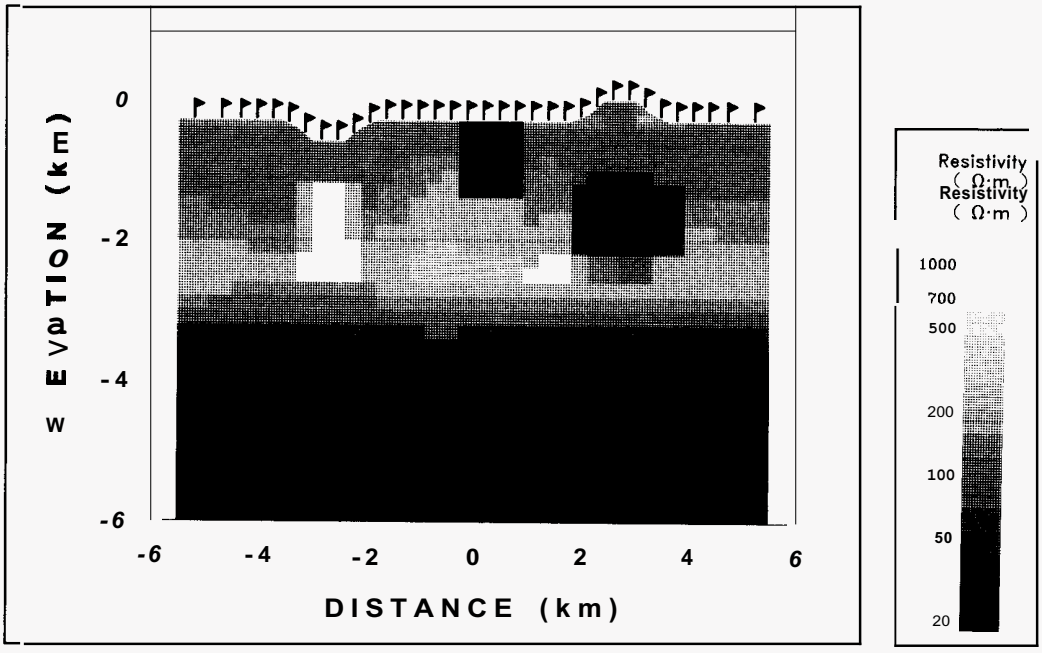

Figure **4.** Inverted result of synthetic TM mode data

traverse. The 300m spacing between the MT sites allows for investigation of the deep geoelectric structure.

In the CSMT survey scalar measurements were made with the electric field oriented along the traverse and the magnetic field normal to traverse. For the frequency range of 1,024Hz to 64 Hz the source is sufficiently far away that the plane-wave approximation is valid in the inversion algorithm. In MT surveys the clcctric field is typically measured over a frequency range of about 0.01-250Hz using grounded electric dipoles, oriented orthogonally to and normal to the traverse. The magnetic field is measured over the same frequency range with three coils: one vertical coil and two horizontal coils oriented parallel to and normal to the traverse direction. Figures 6 and 7 show the inversion images of line C and line I These profiles are almost the same. Surface resistive layers may be correlated with the Quaternary lava. Underneath this resistive layer, conductive features are found at 500-700m. These can be attributed to the abundant presence of clay minerals due to hydrothermal alteration.

The uplift of the resistive basement in Figures 6 and 7 may be recognized in the western part of each line. This feature may be associated with fault structures This fault has

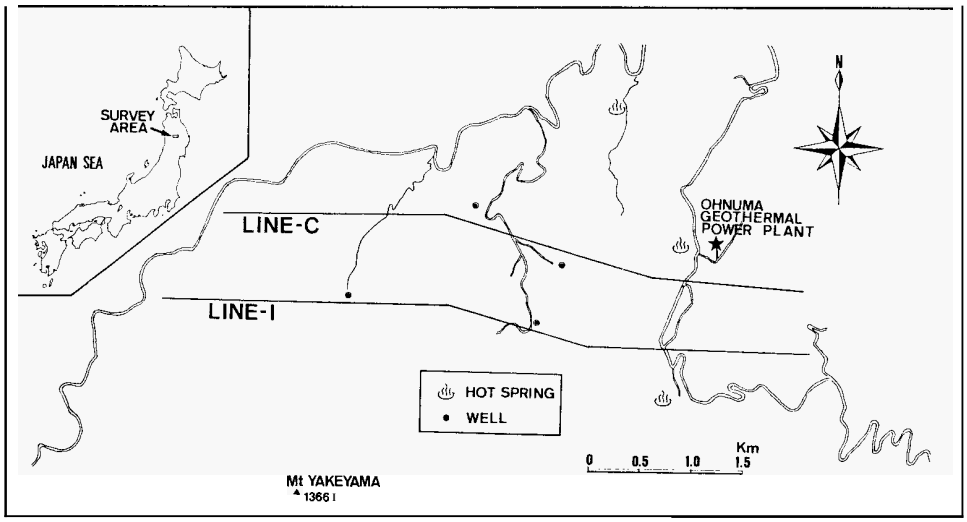

Figure 5 Location map showing the positions and onentations of the two the CSMT/MT lines

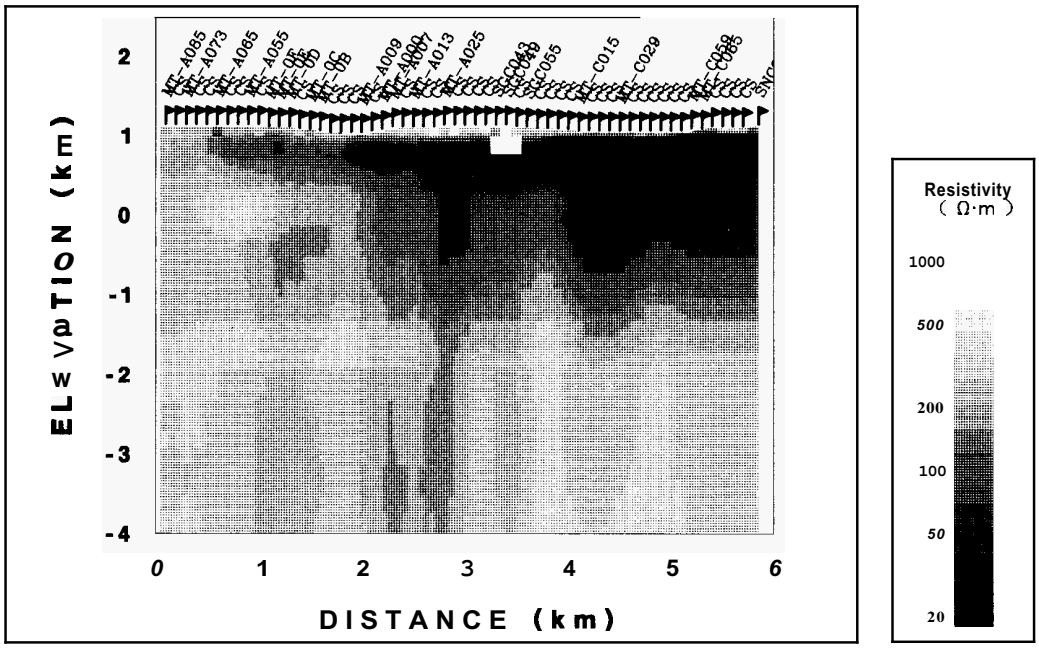

Figure 6. Cross section profile of 2-D inversion in line C

surface manifestations and its existence is also supported by drill-hole data

Conclusions

The GRRI algorithm offers a new way to directly convert MT data acquired over rough terrain with variable topography into subsurface imagcs. It is possible to reconstruct these resistivity images with a rclatively small amount of computer resources.

When compared with the original RRI method, the GRRI method docs not require additional computation timc, and the inverted imagc has higher resolution because the new scheme is bascd on a locally two-dimension analysis.

Finally, the GRRI mcthod has been successfully tested with both synthetic and field data over variable terrains. The rcsults arc reasonably acceptable.

Acknowledgments

This work was supported by the New Energy and Industrial Technology Development Organization (NEDO). The CSMT survey was conducted by Bishimetal Exploration Co., Ltd , who also developed a new data-acquisiton system, GDP-32NJ, with Zonge Engineering & Research Organization of Tucson, AZ as part of NEDO project. Also, we wish to thank T. H. Asch Ph.D. for his assistance in writing the code.

References

deGroot-Hedlin., C., and Constable. S., (1990). Occam's inversion to generate smooth, two-dimensional models from magnctotclluric data, : *Geophysics*. Vol. 55, pp1613-1624.

Smith, J.T. and Booker, J. R. (1991) Rapid Inversion of Two- and Three Dimensional Magetotelluric data: *J. Geophy. Res* , Vol. 96, pp3905-3922

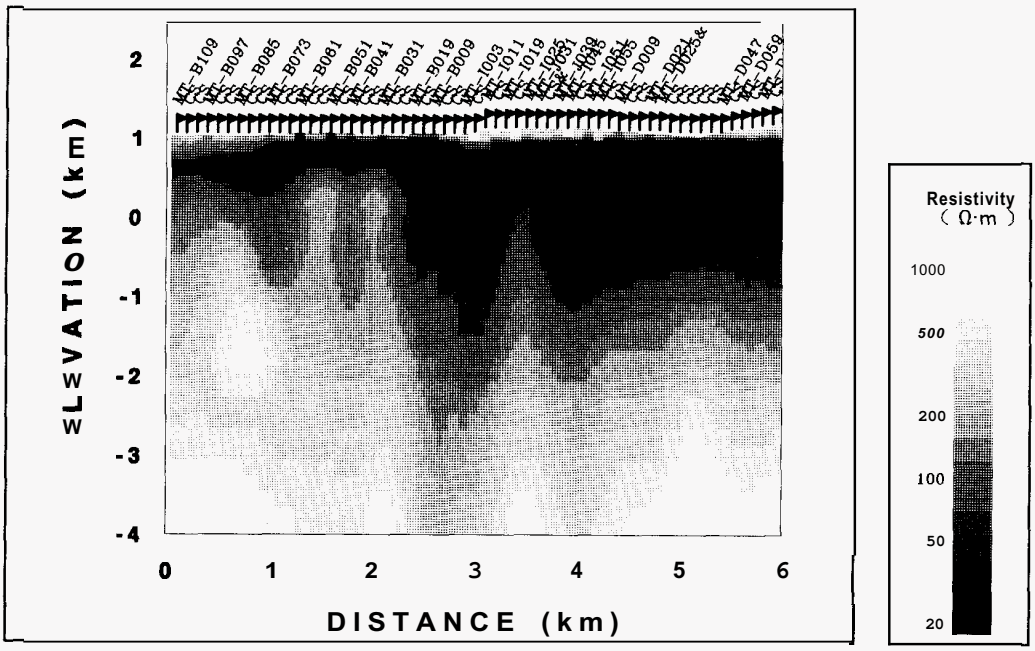

Figure 7. Cross section profile of 2-D inversion in line I